Biochemical and Biophysical Research Communications

Von-Hippel Lindau protein amyloid formation. The role of GST-tag.

--Manuscript Draft--

Manuscript Number:	BBRC-24-3338
Article Type:	Short Communication
Keywords:	amyloid fibrils, physiological amyloids, membrane-less organelles; A-bodies; intrinsically disordered proteins; protein aggregation
Corresponding Author:	Alexander V. Fonin Institute of Cytology Russian Academy of Sciences RUSSIAN FEDERATION
First Author:	Natalia V. Kuzmina
Order of Authors:	Natalia V. Kuzmina
	Anastasiia A. Gavrilova
	Anna S. Fefilova
	Anna E. Romanovich
	Irina M. Kuznetsova
	Konstantin K. Turoverov
	Alexander V. Fonin

Corresponding author:
Dr. Alexander V. Fonin
Laboratory of Structural Dynamics,
Stability and Folding of Proteins,
Institute of Cytology, Russian
Academy of Sciences
4, Tikhoretsky av., St. Petersburg,
194064, Russian Federation
E-mail:
alexfonin@incras.ru

Dear Editor,

With this letter I would like to submit our work “Von-Hippel Lindau protein amyloid formation. The role of GST-tag” by Natalia V. Kuzmina et al. for publication as a Short Communication in Biochemical and Biophysical Research Communications.

Von-Hippel Lindau protein (VHL) is included in the formation of so-called A-bodies, which are the nucleolar physiological fibrillar formations that arise in response to acidosis or heat shock. Here we first studied the amyloid fibril formation of VHL and GST-VHL fusion proteins in acidic conditions. It was shown the significant difference between formed by VHL and GST-VHL. It is established that GST-tag catalyzes VHL amyloid fibril formation, superimpose chirality, increases length and level of hierarchy, but decreases rigidity of amyloid fibrils. The obtained data indicate that tagging can significantly affect the fibrillogenesis of the target protein.

Currently, the manuscript comprises 4032 words in the text (including title page, references, and figure legends) and 3 figures

With best regards,
Alexander V. Fonin

Highlights

1) We first performed AFM-study of fibrils formed by VHL protein and by VHL fused with GST-tag at acidic conditions
2) VHL forms short heterogenic fibrils with persistent length of 2.400 nm and average contour length of 409 nm
3) GST-tag catalyzes VHL amyloid fibril formation, superimpose chirality, increases length and level of hierarchy, but decreases rigidity of amyloid fibrils

Von-Hippel Lindau protein amyloid formation. The role of GST-tag.

Natalia V. Kuzmina [1], Anastasia A. Gavrilova [2], Anna S. Fefilova [3], Anna E. Romanovich [4], Irina M. Kuznetsova [2], Konstantin K. Turoverov [2], Alexander V. Fonin [2,*]

[1] A.N. Frumkin Institute of Physical Chemistry and Electrochemistry, Russian Academy of Sciences, Bldg. 4, 31, Leninskiy ave., 119071, Moscow, Russia

[2] Laboratory of Structural Dynamics, Stability and Folding of Proteins, Institute of Cytology, Russian Academy of Sciences, 4 Tikhoretsky Ave., 194064 St. Petersburg, Russia

[3] Center of Genomic Regulation (GRC), Barcelona Institute of Science and Technology, Barcelona, 08003, Spain

[4] Resource Center of Molecular and Cell Technologies, St-Petersburg State University Research Park, Universitetskaya Emb. 7-9, 199034 St. Petersburg, Russia

* Correspondence: alexfonin@incras.ru (A.V.F.)

Abstract: In the last decade, much attention is given to study of physiological amyloid fibrils. These structures include A-bodies, which are the nucleolar fibrillar formations that appear in response to acidosis and heat shock, and disassemble after the end of stress. One of the proteins involved in the biogenesis of A-bodies, regardless of the type of stress, is Von-Hippel Lindau protein (VHL). Known also as a tumor suppressor, VHL is capable to form amyloid fibrils both *in vitro* and *in vivo* in response to environment acidification. As for majority of amyloidogenic proteins fusion with different tags is used for increase of VHL solubility. Here, we first performed AFM-study of fibrils formed by VHL protein and by VHL fused with GST-tag (GST-VHL) at acidic conditions. It was shown that formed by full-length VHL fibrils are short heterogenic structures with persistent length of 2.400 nm and average contour length of 409 nm. GST-tag catalyzes VHL amyloid fibril formation, superimpose chirality, increases length and level of hierarchy, but decreases rigidity of amyloid fibrils. The obtained data indicate that tagging can significantly affect the fibrillogenesis of the target protein.

Keywords: amyloid fibrils, physiological amyloids, membrane-less organelles; A-bodies; intrinsically disordered proteins; protein aggregation

1. Introduction

Amyloid fibrils have been intensively studied for more than 100 years [1]. In the last decade, special attention has been paid to the physiological amyloid fibrils that are structures having cross β-sheet topology but do not have a toxic effect on cells and have pronounced functional activity [2]. Proteins involved in the biogenesis of such structures include Von-Hippel Lindau protein (VHL) is known as a tumor suppressor, encoded by *VHL* gene. VHL is included in regulation of many cellular processes via interaction with different factors in direct or indirect forms [3,4]. In particular, VHL is involved in the formation of so-called A-bodies, which are the nucleolar fibrillar formations that arise in response to acidosis or heat shock [5]. The signal for the formation of A-bodies is transcription from the intergenic spacer (IGS) part of rDNA, enriched in dinucleotide repeats [6]. In turn, synthesized rIGSRNAs induce nucleolar sequestration some proteins, including VHL and their subsequent fibrillization [7]. On the other hand, VHL forms a ternary complex with elongin B and elongin C, and serves as substrate recognition subunit for E3 ligase protein complex [8]. This complex provides ubitiquination and degradation of hypoxia-inducible transcription factors (HIFs) involved in cell response to oxygen levels. Recent study of Kumar et al. suggested VHL amyloid form-mediated regulation of HIFs under stress conditions. Authors revealed inherent tendency of VHL to form amyloids under native-like conditions and related it with protein function regulation via switching to an inactive form resistant to proteolytic cleavage and degradation [9].

Structurally VHL possesses intrinsically disordered nature, which provide high propensity for aggregation [3]. Several regions have been identified in the protein sequence with high propensity to form β-sheet rich aggregates. Kumar et al. reported of six aggregation-prone and amyloidogenic segments of VHL based on in-silico predictions. Further investigation of corresponding peptides showed the enhancement in the ThT fluorescence at aggregation for two of them, namely ^{72}SQVIFCN^{78} and ^{147}IFANITL^{153}, called SN7 and IL7 respectively. AFM and EM study of the peptide's aggregates revealed that amyloids of SN7 appear as clusters of intercalated fibrils with a height of 5-10 nm and of diameter ~30 nm while IL7 amyloids were observed to be separated rod-shaped mature fibrils of 3-13 nm height, ~46 nm diameter and varying length [10]. It was shown that the VHL104-140 fragment with arginine/histidine cluster in close proximity to a highly amyloidogenic stretch of amino acids is responsible for VHL sequestration to A-bodies [5].

As the majority of amylodogenic proteins, VHL is difficult to obtain when it is heterologously expressed. So, recombinant His-tagged VHL from inclusion bodies formed in *E. coli* cells, and refolded after showed high propensity for amyloid aggregation when incubated in PBS (pH 7.4) at 37 °C for 72 h [9]. Nevertheless, VHL fibrils structure and properties formed under native-like and acidic conditions still remain uncharacterized.

Expression and purification of protein of interest via recombinant expression include several approaches. Application of the purification tags may provide sufficient yield and high purity of protein of interest while preserving their native structure and function [11]. Glutathione S-transferase (GST-tag) is known to frequently increase the solubility of the fused protein of interest and thus enabling its purification and subsequent functional characterization [12]. Despite widespread utilization of GST tag one have poor understanding of its influence on protein's

amyloid fibrils formation. In the particular study of huntingtin presence of GST tag was reported to prevent fusion protein from high-molecular weight amyloid aggregation, whereas tag cleavage with proteases lead amyloid fibril formation [13] . On the other hand, prionogenic peptide derived from Sup35 was revealed to force the whole fusion protein to show amyloid characteristics [14]. This effects look contradicting and remain the role of GST tag in amyloid aggregation speculative.

Here we investigated amyloid fibril formation of both VHL and GST-VHL fusion proteins.

Materials and methods

pGEX2TK plasmid (Addgene #20790) encoding for the GST-VHL was used to transform E. coli BL21(Rosetta 2) cells. The expression of the protein was then induced by adding 0.5 mM isopropylbeta-D-1-thiogalactopyranoside (IPTG; Sigma, USA). Recombinant protein was subsequently purified using GST-GraviTrap, Superose 12 and monoQ columns (GE Healthcare, Chicago, IL, USA). Protein purification was controlled using denaturing SDS-electrophoresis in 15% polyacrylamide gel. GST tag elimination was performed by thrombin (GE Healthcare, Chicago, IL, USA and subsequent ion-exchange chromatography (monoQ, GE Healthcare, Chicago, IL, USA).
Incubation of protein solution at 37°C was carried using Binder B 28 thermostat (Binder GmbH, Tuttlingen, Germany) out in 20 mM Tris-HCl, 150 mM NaCl buffer, pH value was adjusted by addition of appropriate volume of HCl. Then samples were prepared for AFM imaging. A freshly cleaved mica slice was placed on top of a 20 μL VHL protein solution and left for adsorption for 5 minutes. After that surface was rinsed with 1 ml of deionized water and dried in air flow. AFM experiments were carried out using Nanoscope V multimode atomic force microscope (Veeco Instruments, Santa Barbara, California) in tapping mode in air. Commercial super sharp high resolution NSG30_SS (spring constant 40 N/m, resonance frequency 320 kHz) silicon cantilevers (Tipsnano, Tallinn, Estonia) with tip curvature radius of 2nm were used. The scan rate was typically 2 Hz. Image processing was performed using FemtoScan Online software (Advanced Technologies Center, Russian Federation) [15-18].

Calculation of persistent length was carried out within worm-like chain model based on the distribution of the angle between the tangents to the contour of the molecule in the open-source FiberApp program [19].

Results and discussions

Incubation of GST-VHL at pH 2 during 2 weeks

GST-VHL fusion protein incubated in a solution with acidic pH (pH 2) at 37°C during 2 weeks showed the presence of various fibrillar structures as well large aggregates. The length of the fibrils ranges from 200 nm to 20.7 microns, and the height corresponding to diameter varies from 1.2 nm to 35 nm. Structures formed at acidic conditions of pH 2 are hierarchical: two or more fibrils wind together resulting in thicker fibrils with increasing diameter. Figure 1B represents general field of view with fibrils of various diameters, cyan arrow point to intertwining of at least 12 particular

fibrils into a thicker one. Panel C shows individual zoom-in areas of intertwining fibrils. Accompanying large aggregates indicated with magenta arrows at Figure 1B are of various sizes and rounded shape with height of more than 130 nm. Large aggregates morphology is quite often include a bunch of protruding fibrils as clearly visible at panel D.

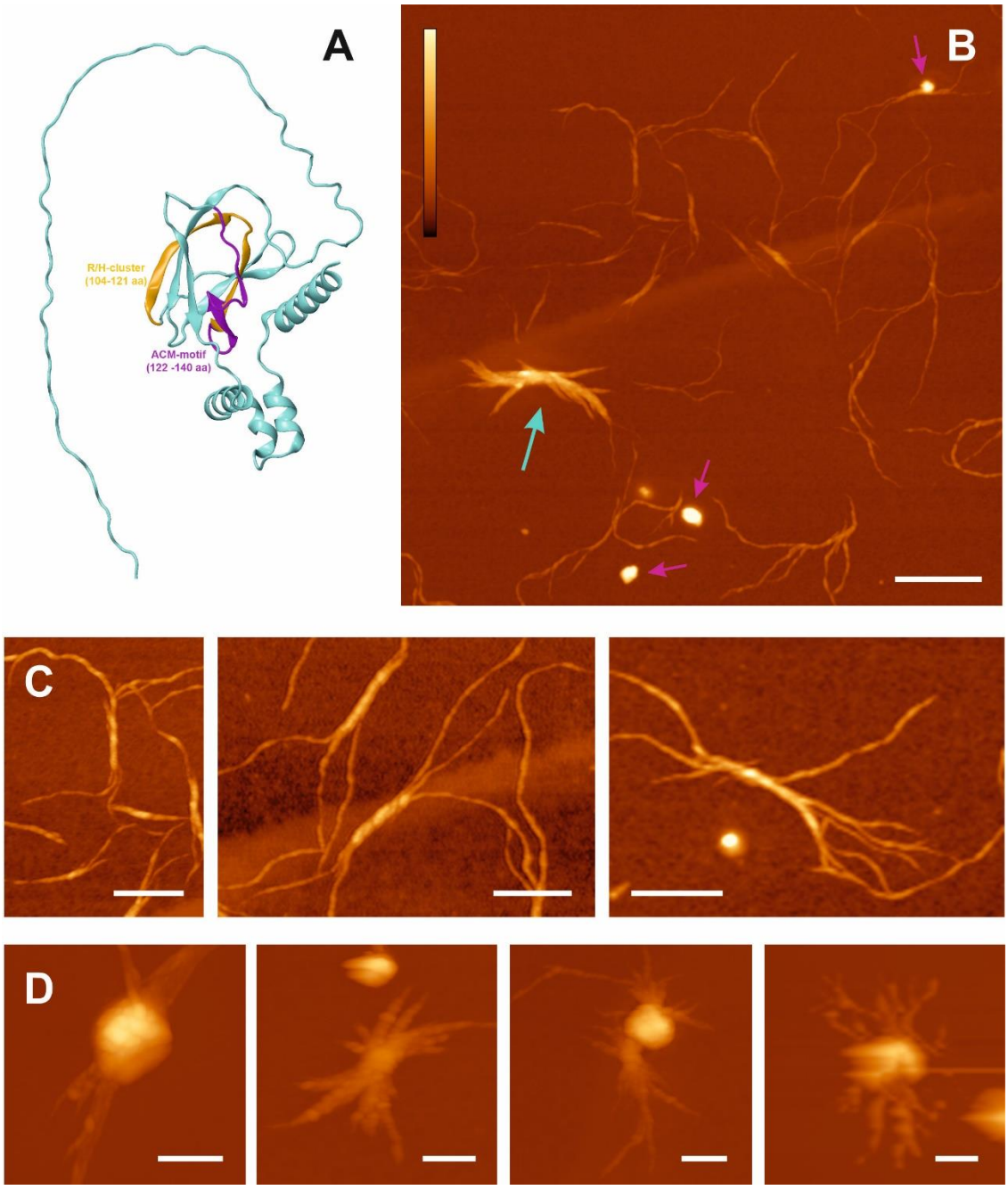

Figure 1. GST-VHL amyloid fibril formation

A) VHL structure predicted using AlphaFold2 [20]. R/H cluster (104-121 aa) and ACM-motif are highlighted by orange and purple colors, respectively. B) AFM image of GST-VHL structures formed upon incubation at pH 2 at 37°C during 2 weeks. Scale bar In XY is 1 micron, in Z is 55 nm. C) Zoom-ins of GST-VHL fibrils constituting of

various number of protofibrils. Scale bar In X is 400 nm, in Z is 20 nm. D) Zoom-ins of GST-VHL large aggregates with associated fibrils. Scale bar In XY is 400 nm, in Z is 200 nm.

Storage of fusion protein solution at + 6°C during 2 weeks resulted in abrupt increase in mass content of large aggregates by an order of magnitude, along with fibrillar structure content oppositely fell down. This may indicate to the pathway of amyloidosis from partially unfolded VHL protein to amyloid plaques through fibrillar structures [21]. Incubation of GST-VHL at the solution with pH 4 also resulted in complex hierarchy of fibrils with height ranging from ~ 1 nm up to 28 nm. However, we haven't observed fibrils longer than 700 nm, neither large aggregates resembling amyloid plaques were revealed for the case of pH 4.

Similar acidification related elongation of amyloid fibrils was reported for TTR (105−115) fibrils: the average length of fibrils formed at pH 2.5 was much shorter than that at pH 1.5.

This may be explained by usually accepted paradigm that the process of amyloid fibril formation commences from partially unfolded structure of proteins which induces with environment acidification. Decreasing of pH to very acidic conditions gives rise to specific intermolecular interactions such as hydrogen bonding, electrostatic, and hydrophobic interactions which can drive fibril formation [22].

Incubation of VHL at pH 2 during 2 weeks

VHL protein revealed much lower propensity to amyloid fibrils formation than GST-VHL fusion protein. Figure 2A demonstrates the result of VHL incubation at pH 2 at 37 °C without any stirring during 2 weeks: observed fibrils are short with length up to 300 nm and height up to 8 nm. The same pH and temperature with constant stirring of protein solution during incubation led fibril's length and height to increase, which grew up to 1750 nm long and up to 28 nm high (shown at Figure 2B). Maximum length value by an order of magnitude is shorter than those for GST-VHL. Average length for VHL protein fibrils of 409 nm is far smaller than one of GST-VHL of 2.700 nm. Morphology of mature VHL fibrils is non-uniform along the axis: fibrils look like as if partially unfolded protein multimers together with partially unfolded monomers participate in mature fibril formation possibly via cross-beta-spin or domain-swapping mechanism [23]. GST-VHL fusion protein mature fibrils exhibit uniformity along the axis and high level of hierarchy where intertwining of protofibrils play dominant role in mature fibrils formation. Such difference in the morphology of GST-VHL and VHL mature fibrils is quite intriguing. Generally, nucleation-elongation mechanism of amyloid fibril formation implies preceding stage of amyloidogenic seeds (oligomeric form) of the protein. For VHL protein we observed numerous globular particles of various height and diameter, which possibly represent amyloidogenic seeds. Our suggestion, that VHL may provide diverse range of populations of seeds upon environment acidification, which may interact with each other to form fibril. However, it may be less favourable for fibril growth due to some reasons (as steric constrains or electrostatic repulsion) in comparison with interacting of identical seeds. It should be noted, that amyloid fibrils formed by peptides localized in ordered C-terminal domain of VHL (SN7 (72-78 aa), IL7 (147-153 aa), ACM (122-140 aa)) have

morphology closed to GST-VHL fibrils [5,9,10]. From this point, GST tag positioning at the disordered N-terminus of VHL protein may prevent from the formation of diverse populations of seeds, making them identical and providing rapid fibril growth.

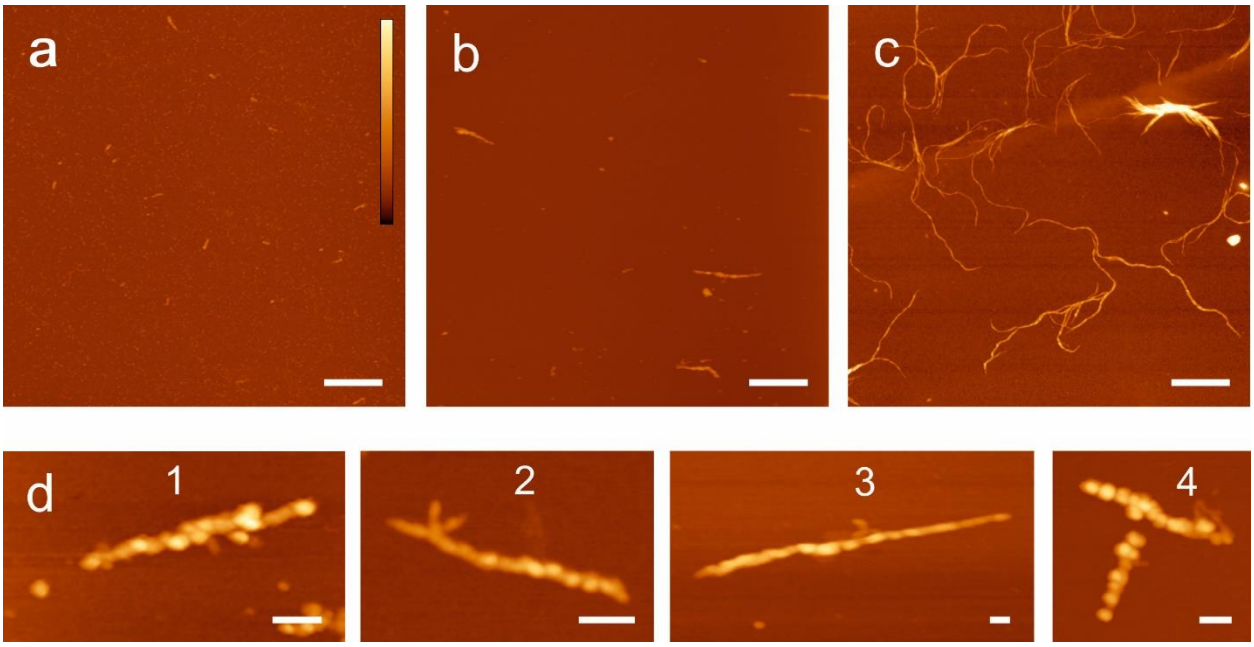

Figure 2. VHL and GST-VHL amyloid fibril formation at pH 2. AFM images of a) VHL upon incubation at pH 2 at 37°C during 2 weeks; b) VHL upon incubation at pH 2 at 37°C during 2 weeks with constant stirring c) GST-VHL upon incubation at pH 2 at 37°C during 2 weeks with constant stirring. Scale bars for a-c in XY are 1 μm, in Z 30 nm. d) Zoom-ins of VHL fibrils presented on Panel b. Scale bar in XY is 100 nm, in Z is 14 nm for 1, 2, 3 and 30 nm for 4.

Chirality

As described previously presence of GST tag on VHL protein change resulting mature fibril morphology so that VHL fibrils represent beads of various sizes on a rod, while GST-VHL fibrils are mostly uniform along the axis with clearly visible period and twist. According to this we were able to resolve the chirality only for the fusion protein. GST-VHL fibrils at pH 2 revealed the dominance of left handedness (90%) at all hierarchy levels, though 10 % showed right-handedness. Literature analysis of amyloid fibril chirality of various proteins incubated at up to 37°C displayed at Table 1. As one can see both handedness coexists under the same incubation conditions. This may indicate that chirality is not only determinated by amino acid sequence of the protein but rather by local environmental changes; or coexistence of left- and right-handedness related with changing chirality upon transition to another level of hierarchy like was shown for albumin (upon heating at 90°C and pH 2) by Usov et. al [24]. In our case of GST-VHL fibrils the dominance of left-handed fibrils grown up at pH 2 was observed for all levels of hierarchy and we haven't find any correlation between fibrils thickness, number of protofibrils constituting mature fibrils and chirality.

Table 1. Chirality of amyloid fibrils formed by different proteins incubated at temperatures up to 37°C

Protein	Incubation conditions	handedness
IAPP [25]	milliQ	both left- and right-handed morphologies with different periodicities
receptor-interacting protein kinases 3 (RIPK3) [26]	6 M Guanidine hydrochloride, 50 mM Tris·HCl [pH 8.0], 50 mM sodium chloride, 500 mM imidazole, and 2 mM dithiothreitol	71.9 % left-handed and to 28.1 right-handed
wild-type α-synuclein [27]	25 mM Na-PO4, pH 6.2, 0.02% NaN3 at 37°C	right-handed fibrils and left-handed fibrils
α-syn**uclein** (wildtype and the three mutants A30P, E46K and A53T) [28]	incubated at 37 ºC in 10 mM HEPES, 50 mM NaCl, pH 7.4 under constant stirring at 300 rpm in glass vials	WT fibrills are right-handed according to pictures, fibrills of mutants are both right- and left-handed
α -synuclein [29]	pH 6	right-handed fibrils with periodicities of ~ 45 nm and left-handed fibrils with periodicities of ~ 95 nm.
glucagon [30]	agitated at 37°C pH 2	both right-handed and left handed fibrils with dominance of right-handedness according to presented images

Incubation of GST-VHL at pH 4 resulted in fibrils less uniform along the axis but still having segments with twisted morphology. All resolved fibril handedness for the case of pH 4 were right (Fig. 3b). Tuning of chirality by pH have been described by Kurouski et al in the study of 5 particular protein and peptide fragments [31]. Authors report that pH dependence of chirality for proteins insulin, lysozyme, and apo-α-lactalbumin (reversed, right-handed at lower pH and normal, left-handed at higher pH) is opposite to the case of the peptide fragments HET-s (218−289) from prion protein, and TTR (105−115) from transthyretin (normal, left-handed at lower pH and reversed right-handed at higher pH) [31]. Handedness inversion in all cases was observed at pH~2, possibly due to protonation/deprotonation of amino acid residues, changing the charge on the surface of the protofilaments, as well changing in the hydrophobic-hydrophilic local environment leading protofilaments to reverse their gradual twist. Subsequent protofilaments with opposite handedness may result in different mature fibrils formation mechanisms.

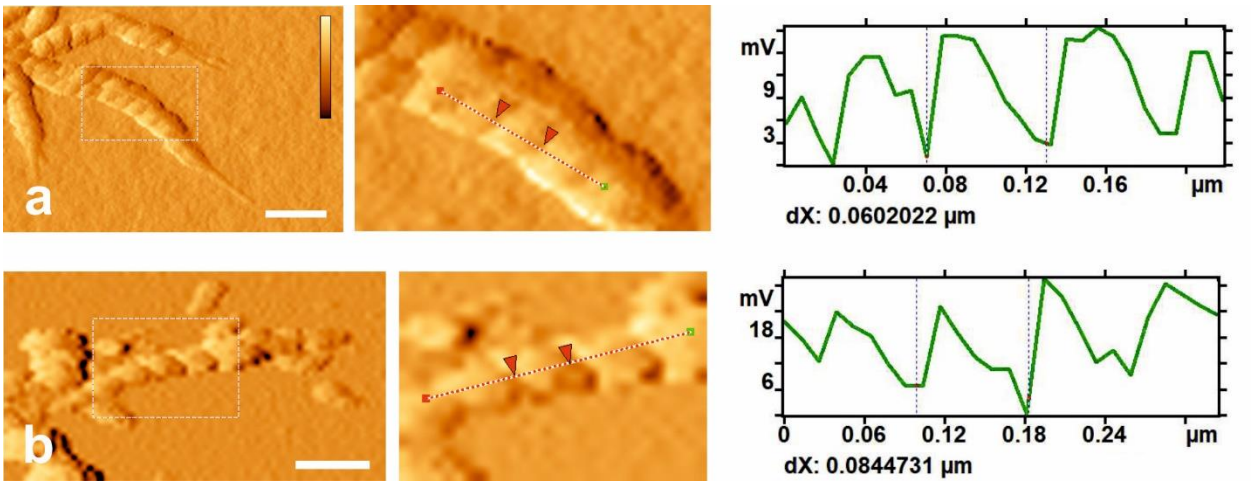

Figure 3. GST-VHL amyloid fibril formation at different pH.

a) AFM phase image of GST-VHL upon incubation at pH 2 at 37°C during 2 weeks, zoom-in of selected area and corresponding profile of drawn line b) AFM phase image of GST-VHL incubated at pH 4 during 2 weeks, zoom-in of selected area and corresponding profile of drawn line. Scale bars in X are 200 nm.

Persistent length

Analysis of amyloid fibrils flexibility was carried out based on polymer physics formalism. We used worm-like chain model to calculate the persistent length lp, at which the polymer begins to bend in different directions due to thermal fluctuations. Formally the persistent length is the length at which angular correlations in the tangent directions along the polymer are decreased on average by e times. The persistent length characterizes the flexibility of the polymer, usually the analysis of the stiffness or elasticity of molecules is carried out by comparing the persistent and contour lengths. A fibril is considered to be flexible when $lp \ll L$ and rigid when it opposite ($lp \gg L$) [22]. Persistent length of GST-VHL protein fibrils formed in a solution with pH 2 turned out to be (976 ± 10) nm, which, taking into account the contour lengths described above (average contour length 2.7 µm), indicates a quasi-flexible character of the studied fibrils. At the same time persistent length of VHL protein fibrils of (2.5 ± 0.2) µm considering average contour length of 409 nm show more rigid nature compared to that of chimeric GST-VHL.

Conclusions

Here we characterized the structures formed by VHL protein upon environment acidification. VHL provides diverse amyloidogenic seeds interacting with each other and forming mature fibrils as beads of various sizes on a rod. This phenomenon, from our point of view, may be related with disordered N-terminus of the protein. Broad ensemble of protein conformational states increases the number of amyloidogenic seed types and decreases the rate of fibril growth. Fusion of VHL with GST tag at the N-terminus restrict the number of seed's populations: high amount of identical seeds drives rapid fibril's growth characterized by uniformity along the axis, long length, possession of chirality and high level of hierarchy. Also, according to measured persistent length, GST tag significantly reduces mature amyloid fibril's stiffness. Our hypothesis is confirmed by

the fact that amyloid fibrils, formed by peptides localized in the ordered C-terminal domain of VHL (SN7 (72- 78 aa), IL7 (147-153 aa), ACM (122-140 aa)) have a morphology close to GST-VHL fibrils [5,9,10].

Funding: This research was funded by Russian Science Foundation, grant number 21-75-10166 (A.V.F.).

References

[1] J.D. Sipe, A.S. Cohen, Review: history of the amyloid fibril, J Struct Biol 130 (2000) 88-98. 10.1006/jsbi.2000.4221.
[2] J.B. Woodruff, A.A. Hyman, E. Boke, Organization and Function of Non-dynamic Biomolecular Condensates, Trends Biochem Sci 43 (2018) 81-94. 10.1016/j.tibs.2017.11.005.
[3] H. Sutovsky, E. Gazit, The von Hippel-Lindau tumor suppressor protein is a molten globule under native conditions: implications for its physiological activities, J Biol Chem 279 (2004) 17190-17196. 10.1074/jbc.M311225200.
[4] S. Gläsker, E. Vergauwen, C.A. Koch, A. Kutikov, A.O. Vortmeyer, Von Hippel-Lindau Disease: Current Challenges and Future Prospects, Onco Targets Ther 13 (2020) 5669-5690. 10.2147/OTT.S190753.
[5] T.E. Audas, D.E. Audas, M.D. Jacob, J.J. Ho, M. Khacho, M. Wang, J.K. Perera, C. Gardiner, C.A. Bennett, T. Head, O.N. Kryvenko, M. Jorda, S. Daunert, A. Malhotra, L. Trinkle-Mulcahy, M.L. Gonzalgo, S. Lee, Adaptation to Stressors by Systemic Protein Amyloidogenesis, Dev Cell 39 (2016) 155-168. 10.1016/j.devcel.2016.09.002.
[6] M. Wang, X. Tao, M.D. Jacob, C.A. Bennett, J.J.D. Ho, M.L. Gonzalgo, T.E. Audas, S. Lee, Stress-Induced Low Complexity RNA Activates Physiological Amyloidogenesis, Cell Rep 24 (2018) 1713-1721 e1714. 10.1016/j.celrep.2018.07.040.
[7] D. Marijan, R. Tse, K. Elliott, S. Chandhok, M. Luo, E. Lacroix, T.E. Audas, Stress-specific aggregation of proteins in the amyloid bodies, FEBS Lett 593 (2019) 3162-3172. 10.1002/1873-3468.13597.
[8] X. Liu, G. Zurlo, Q. Zhang, The Roles of Cullin-2 E3 Ubiquitin Ligase Complex in Cancer, Adv Exp Med Biol 1217 (2020) 173-186. 10.1007/978-981-15-1025-0_11.
[9] V. Kumar, V. Kaushik, S. Kumar, S.A. Levkovich, P. Gupta, D. Laor Bar-Yosef, E. Gazit, D. Segal, The von Hippel-Lindau protein forms fibrillar amyloid assemblies that are mitigated by the anti-amyloid molecule Purpurin, Biochem Biophys Res Commun 690 (2024) 149250. 10.1016/j.bbrc.2023.149250.
[10] V. Kumar, G.K.K. Viswanathan, K. Ralhan, E. Gazit, D. Segal, Amyloidogenic Properties of Peptides Derived from the VHL Tumor Suppressor Protein, ChemMedChem 16 (2021) 3565-3568. 10.1002/cmdc.202100441.
[11] M. Mahmoudi Gomari, N. Saraygord-Afshari, M. Farsimadan, N. Rostami, S. Aghamiri, M.M. Farajollahi, Opportunities and challenges of the tag-assisted protein purification techniques: Applications in the pharmaceutical industry, Biotechnol Adv 45 (2020) 107653. 10.1016/j.biotechadv.2020.107653.
[12] F. Schäfer, N. Seip, B. Maertens, H. Block, J. Kubicek, Purification of GST-Tagged Proteins, Methods Enzymol 559 (2015) 127-139. 10.1016/bs.mie.2014.11.005.
[13] E. Scherzinger, R. Lurz, M. Turmaine, L. Mangiarini, B. Hollenbach, R. Hasenbank, G.P. Bates, S.W. Davies, H. Lehrach, E.E. Wanker, Huntingtin-encoded polyglutamine expansions form amyloid-like protein aggregates in vitro and in vivo, Cell 90 (1997) 549-558. 10.1016/s0092-8674(00)80514-0.
[14] Y.K. Chae, K.S. Cho, W. Chun, A prionogenic peptide derived from Sup35 can force the whole GST fusion protein to show amyloid characteristics, Protein Pept Lett 9 (2002) 315-321. 10.2174/0929866023408599.
[15] F.A. Yaminsky I., Sinitsyna O., Meshkov G. , FemtoScan Online software Nanoindustry (2016) 42-46.
[16] Y.I. Akhmetova A., 20 years since FemtoScan shows atoms Nanoindustry (2017) 88-89. 10.22184/1993-8578.2017.72.2.88.89.
[17] Y.I. Filonov A., Akhmetova A., Meshkov G. , FemtoScan Online. Why? , Nanoindustry 11 (2018) 336-342 10.22184/1993-8578.2018.84.5.336.342.
[18] A.A.I. Yaminsky I.V., Meshkov G.B, FemtoScan Online Software and Visualization of Nano-Objects in High-Resolution Microscopy, Nanoindustry 11 (2018) 414–416 10.22184/1993-8578.2018.11.6.414.416.
[19] I. Usov, R. Mezzenga, FiberApp: An Open-Source Software for Tracking and Analyzing Polymers, Filaments, Biomacromolecules, and Fibrous Objects, Macromolecules 48 (2015) 1269-1280. 10.1021/ma502264c.

[20] J. Jumper, R. Evans, A. Pritzel, T. Green, M. Figurnov, O. Ronneberger, K. Tunyasuvunakool, R. Bates, A. Žídek, A. Potapenko, A. Bridgland, C. Meyer, S.A.A. Kohl, A.J. Ballard, A. Cowie, B. Romera-Paredes, S. Nikolov, R. Jain, J. Adler, T. Back, S. Petersen, D. Reiman, E. Clancy, M. Zielinski, M. Steinegger, M. Pacholska, T. Berghammer, S. Bodenstein, D. Silver, O. Vinyals, A.W. Senior, K. Kavukcuoglu, P. Kohli, D. Hassabis, Highly accurate protein structure prediction with AlphaFold, Nature 596 (2021) 583-589. 10.1038/s41586-021-03819-2.
[21] E. Drolle, F. Hane, B. Lee, Z. Leonenko, Atomic force microscopy to study molecular mechanisms of amyloid fibril formation and toxicity in Alzheimer's disease, Drug Metab Rev 46 (2014) 207-223. 10.3109/03602532.2014.882354.
[22] J. Adamcik, R. Mezzenga, Proteins Fibrils from a Polymer Physics Perspective, Macromolecules 45 (2012) 1137-1150. 10.1021/ma202157h.
[23] R. Nelson, D. Eisenberg, Recent atomic models of amyloid fibril structure, Curr Opin Struct Biol 16 (2006) 260-265. 10.1016/j.sbi.2006.03.007.
[24] I. Usov, J. Adamcik, R. Mezzenga, Polymorphism complexity and handedness inversion in serum albumin amyloid fibrils, ACS Nano 7 (2013) 10465-10474. 10.1021/nn404886k.
[25] A. Kakinen, Y. Sun, I. Javed, A. Faridi, E.H. Pilkington, P. Faridi, A.W. Purcell, R. Zhou, F. Ding, S. Lin, P. Chun Ke, T.P. Davis, Physical and Toxicological Profiles of Human IAPP Amyloids and Plaques, Sci Bull (Beijing) 64 (2019) 26-35. 10.1016/j.scib.2018.11.012.
[26] X.L. Wu, H. Hu, X.Q. Dong, J. Zhang, J. Wang, C.D. Schwieters, J. Liu, G.X. Wu, B. Li, J.Y. Lin, H.Y. Wang, J.X. Lu, The amyloid structure of mouse RIPK3 (receptor interacting protein kinase 3) in cell necroptosis, Nat Commun 12 (2021) 1627. 10.1038/s41467-021-21881-2.
[27] J.A. Fauerbach, D.A. Yushchenko, S.H. Shahmoradian, W. Chiu, T.M. Jovin, E.A. Jares-Erijman, Supramolecular non-amyloid intermediates in the early stages of α-synuclein aggregation, Biophys J 102 (2012) 1127-1136. 10.1016/j.bpj.2012.01.051.
[28] M.E. van Raaij, I.M. Segers-Nolten, V. Subramaniam, Quantitative morphological analysis reveals ultrastructural diversity of amyloid fibrils from alpha-synuclein mutants, Biophys J 91 (2006) L96-98. 10.1529/biophysj.106.090449.
[29] W. Hoyer, T. Antony, D. Cherny, G. Heim, T.M. Jovin, V. Subramaniam, Dependence of alpha-synuclein aggregate morphology on solution conditions, J Mol Biol 322 (2002) 383-393. 10.1016/s0022-2836(02)00775-1.
[30] K.L. De Jong, B. Incledon, C.M. Yip, M.R. DeFelippis, Amyloid fibrils of glucagon characterized by high-resolution atomic force microscopy, Biophys J 91 (2006) 1905-1914. 10.1529/biophysj.105.077438.
[31] D. Kurouski, X. Lu, L. Popova, W. Wan, M. Shanmugasundaram, G. Stubbs, R.K. Dukor, I.K. Lednev, L.A. Nafie, Is supramolecular filament chirality the underlying cause of major morphology differences in amyloid fibrils?, J Am Chem Soc 136 (2014) 2302-2312. 10.1021/ja407583r.

Declaration of interests

☒The authors declare that they have no known competing financial interests or personal relationships that could have appeared to influence the work reported in this paper.

☐The authors declare the following financial interests/personal relationships which may be considered as potential competing interests: